GLOBULAR CLUSTERS IN VI[illegible]ANAX

Everywhere

Thomas H. Puzia
Institute of Astrophysics
Pontificia Universidad Catolica

&

The Complex Stellar Systems Team @IA-PUC

Complex Stellar Systems Group

Postdoctoral Fellows

Roberto Muñoz - Next Generation Virgo/Fornax Cluster Surveys (NGVS/NGFS)

Sibilla Perina - Complex Stellar Population SEDs at High Spectral Resolution

Jin-Cheng Yu - HPC and Numerical Simulations of Globular Cluster Evolution

Paul Eigenthaler - Galaxies in Compact Groups and Dense Environments

Mia Bovill - High-Resolution Simulations of Galaxy Clusters and Groups

Adal Mesa-Delgado - High-Resolution Chemical Enrichment & Studies of Proplyds

Graduate and Undergraduate Students

Frederik Schönebeck - High-Resolution Spectroscopy of Star Clusters

Matthew Taylor - Formation and Evolution of Compact Stellar Systems & CenA

Mirko Simunovic - Modeling & Formation Mechanisms of Blue Straggler Stars

Sofia Gallego - Galaxy Clusters & Dynamical Evolution of Star Clusters

Simon Angel - Characterization of Stellar Populations in Deep Survey Fields

Extragalactic Globular Cluster Systems - Formation/Assembly

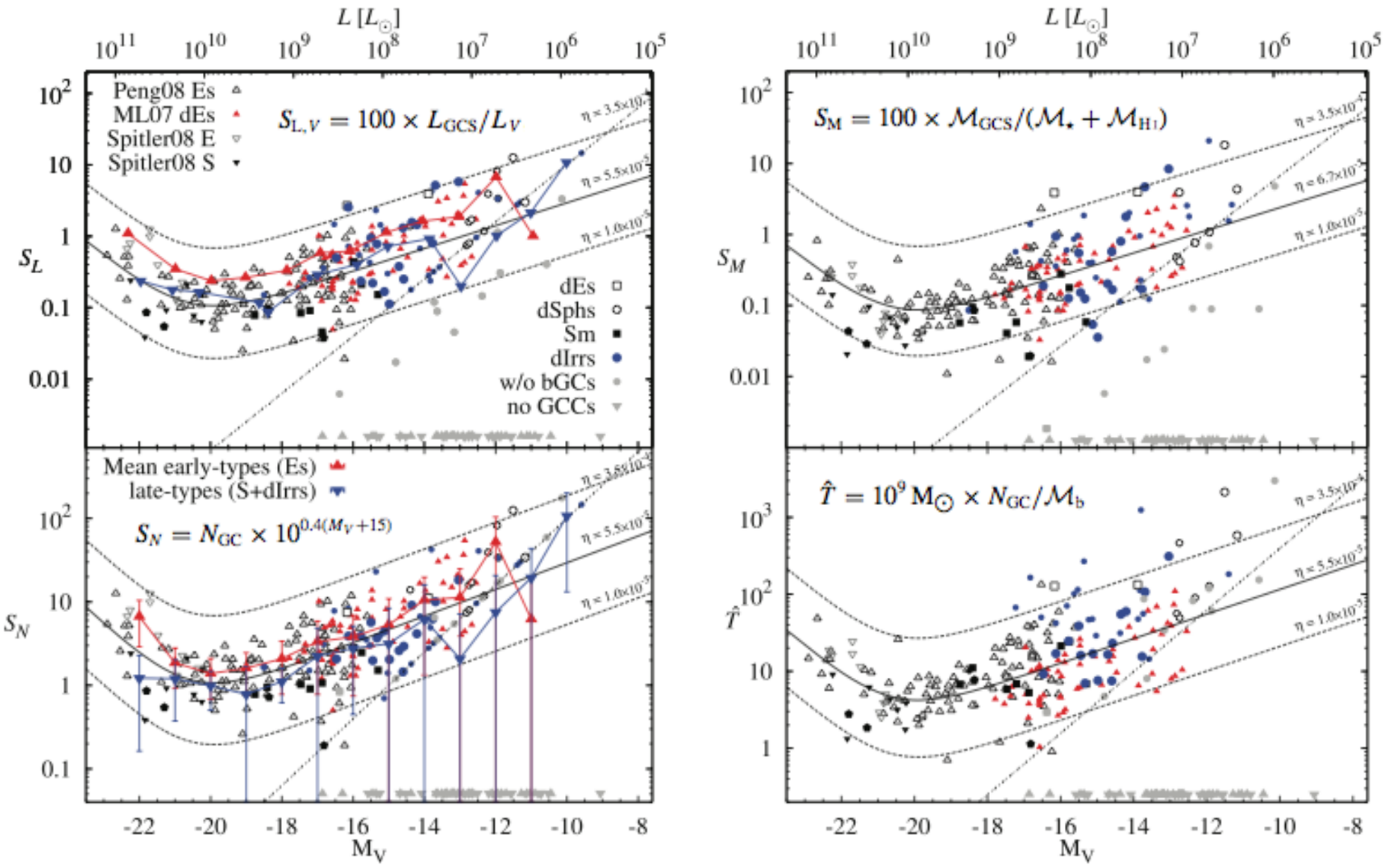

Georgiev et al. (2010)

Figure 6. GCS scaling parameters as a function of galaxy luminosity. From top left to bottom right are shown the GC specific luminosities (S_L), specific mass (S_M), specific frequencies (S_N) and specific number ($\hat{T}$) for all galaxies in the combined sample. Large solid dots indicate dIrrs from our study, while small solid dots are dIrrs from Seth et al. (2004), Sharina et al. (2005) and Georgiev et al. (2006). Solid pentagons show the corresponding values for the Milky Way, M31, LMC and SMC. Grey triangles show galaxies in which no GC candidates are detected. The dash–dotted line represents the corresponding value if the galaxy hosts one GC at present (see Section 4.1). The solid curves are predictions by the models which assume that GCs form proportional to the total galaxy halo mass and that stellar, SNe-driven feedback and virial shock heating regulate galaxy wide star formation (Dekel & Birnboim 2006), below and above $\mathcal{M} \simeq 3 \times 10^{10}\,M_\odot$, respectively (see Section 4.2). The solid curve (top panels) is the best-fitting $\eta_L = 5.5$ and $\eta_M = 6.7 \times 10^{-5}$ value to the S_L and S_M distributions, respectively. The solid lines in the bottom panels are curves with adopted $\eta_L = 5.5 \times 10^{-5}$. Large triangles connected with solid lines in the left-hand panels show the co-added running average S_N and S_L values as a function of galaxy luminosity for early- and late-type systems. Dashed curves illustrate the range in η values among galaxies, between $\eta = 10^{-5}$ and 3.5×10^{-4}.

Extragalactic Globular Cluster Systems - Formation/Assembly

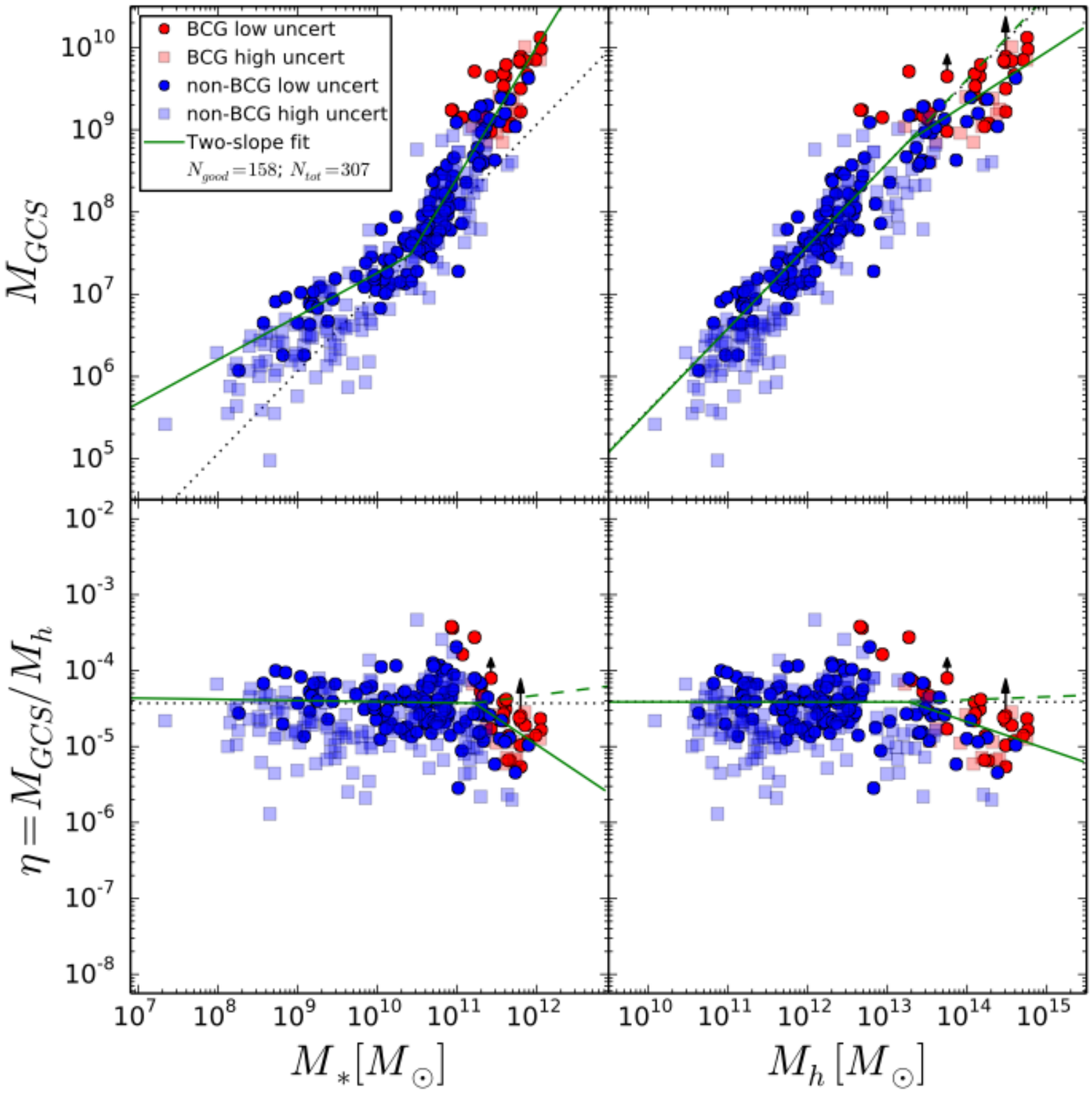

Hudson, Harris (2014)

Extragalactic Globular Cluster Systems - Formation/Assembly

- galaxies are assembled selectively ➠ stellar populations should give answer!

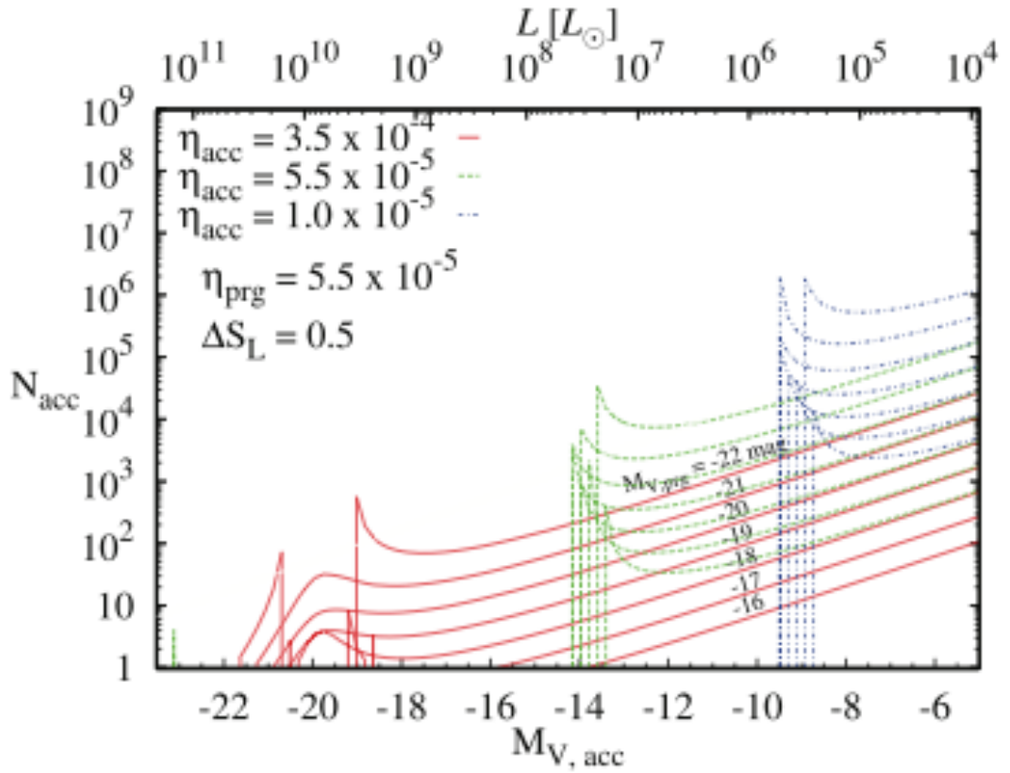

Georgiev et al. (2010)

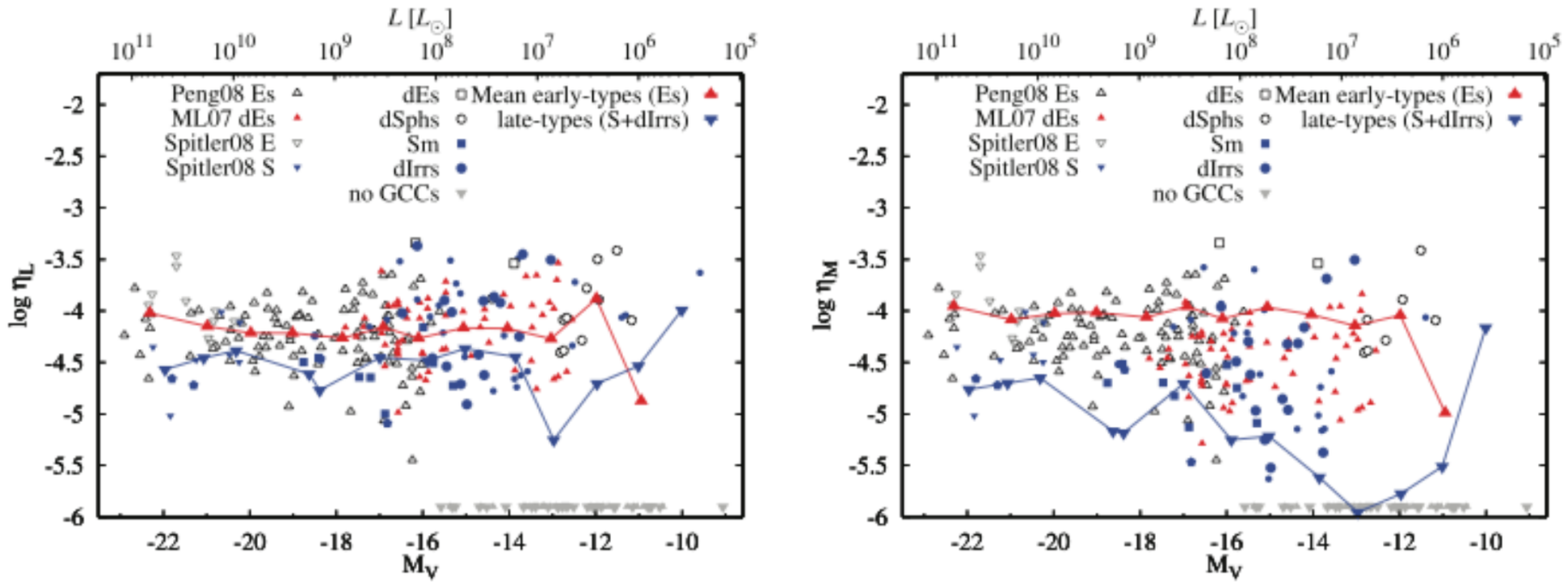

Figure 7. Specific GC formation efficiencies, η, as a function of galaxy luminosity. Left: luminosity-normalized GC formation efficiency (η_L) derived from the S_L relation (equation 24). Right: mass-normalized GC formation efficiency (η_M) derived from the S_M relation (equation 24). The symbols connected with lines show the mean η values (including galaxies without GCCs) in bins of 1 mag. The remaining symbols are as in Fig. 6.

Extragalactic Globular Cluster Systems

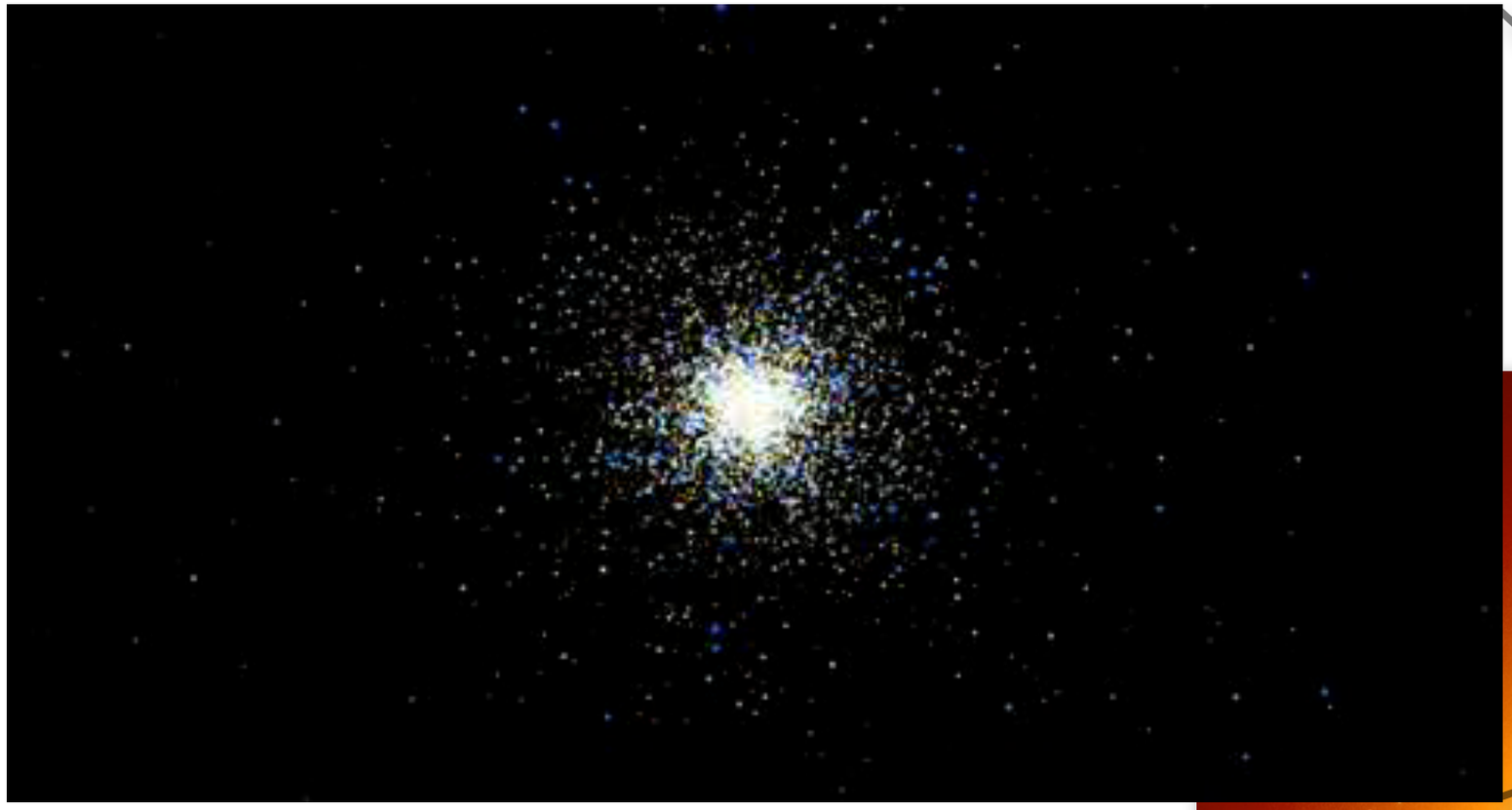

N-body credit: S. Portegies-Zwart

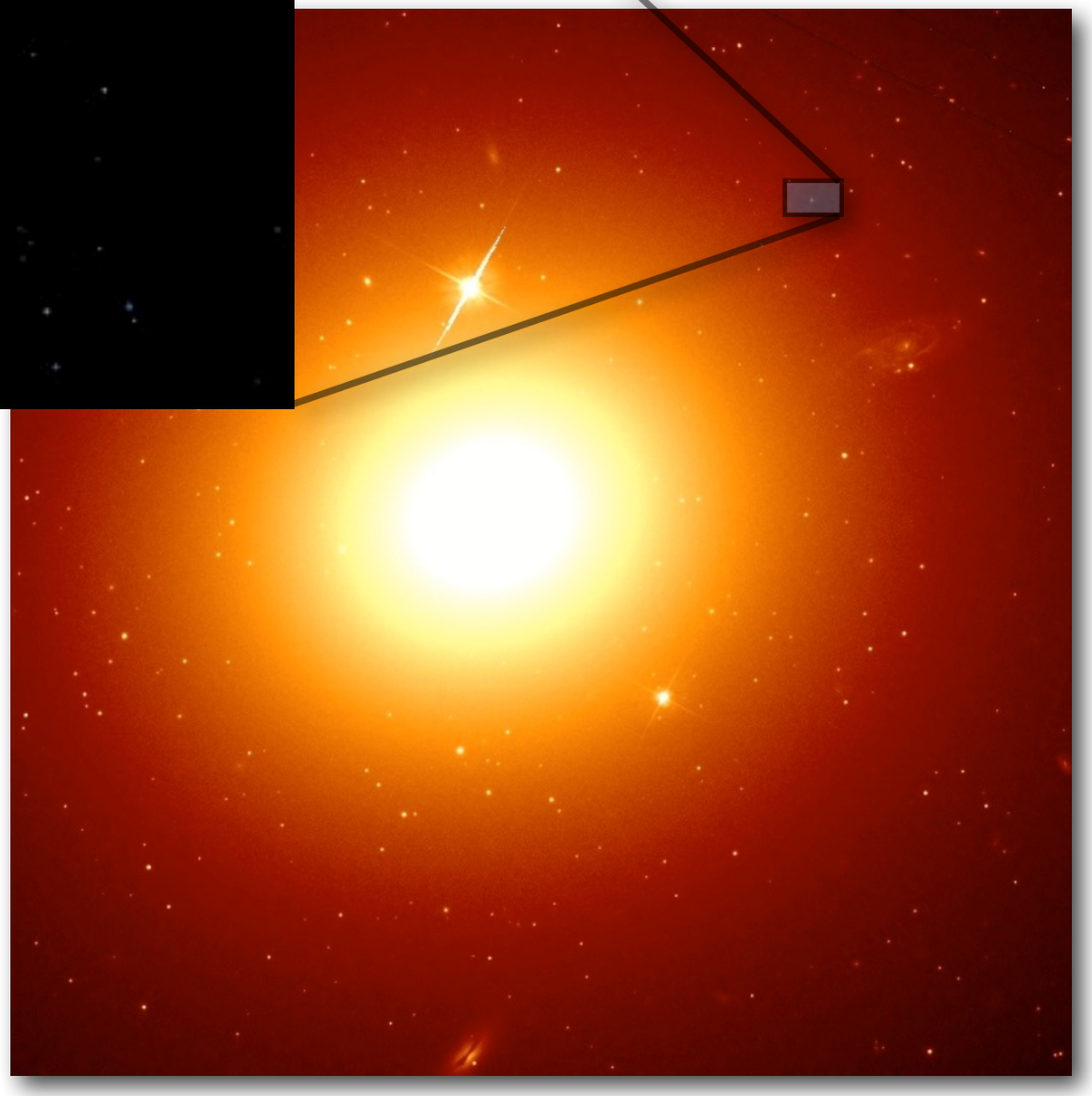

- GCs are oldest stellar systems in the local Universe and best approximations to SSPs
- GCs preserve a snapshot of the detailed chemical mix in their parent environment at the time of their formation
- **GCs respond dynamically to tidal forces at their formation sites and throughout their evolution**

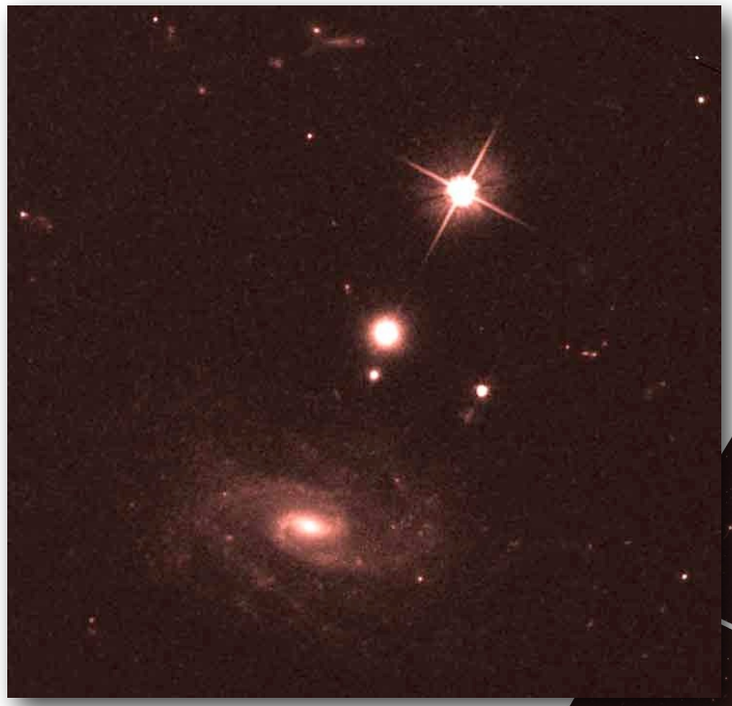

1″ = 97.6 pc
1 pix = 0.03″ = 2.93 pc

1.6 effective radii of the GCS in NGC 1399

10′x10′

Paolillo et al. (2011)
Brescia et al. (2012)
Puzia et al. (2014)

5.7 effective radii of the NGC 1399 diffuse galaxy light

99.053 arcmin^2 observed sky area

Thomas H. Puzia, Institute of Astrophysics, PUC

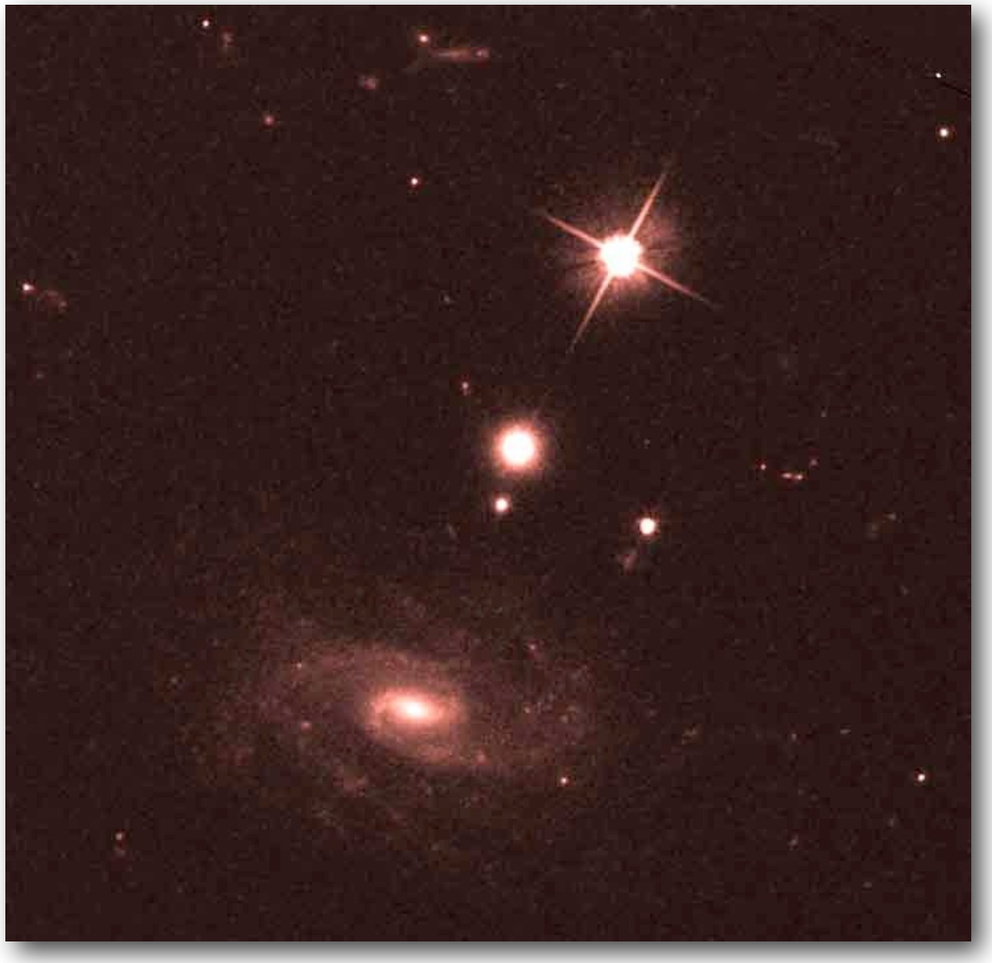

Highest pixel-to-pixel integrity, i.e. lowest fractional pixel spread

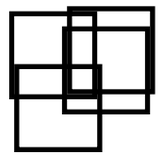

Ok

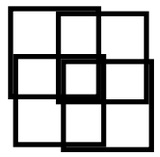

Better!

- For each mosaic tile we used four sub-integrations a 527 sec using a 4-point dither pattern
- F606W filter with total 2108 sec

TABLE 1
PARAMETERS OF THE UTILIZED DITHER PATTERN

Parameter	value
Pattern type	ACS-WFC-DITHER-BOX
Primary pattern shape	PARALLELOGRAM
Pattern purpose	DITHER
Number of points	4
Point spacing	0.285″
Line spacing	0.285″
Coordinate frame	POS-TARG
Pattern orient	30.155 deg
Angle between sides	145.82 deg
Center pattern	NO

66.5% larger than HUDF dither pattern

Puzia et al. (2014)

Building the PSF library

for each tile!

- ACS/WFC PSF is variable across the FoV

- use effective PSF to interpolate local PSF on FLTs

- multidrizzle each mosaic tile using the exact astrometry to combine ePSFs into dePSFs

$$\Sigma(\boldsymbol{r}) = 2\pi \int_{r_1}^{r_2} \{\mu(\boldsymbol{r}) \otimes P(\boldsymbol{r}) \otimes D(\boldsymbol{r}) + N(\boldsymbol{r})\}\, \boldsymbol{r} d\boldsymbol{r}$$

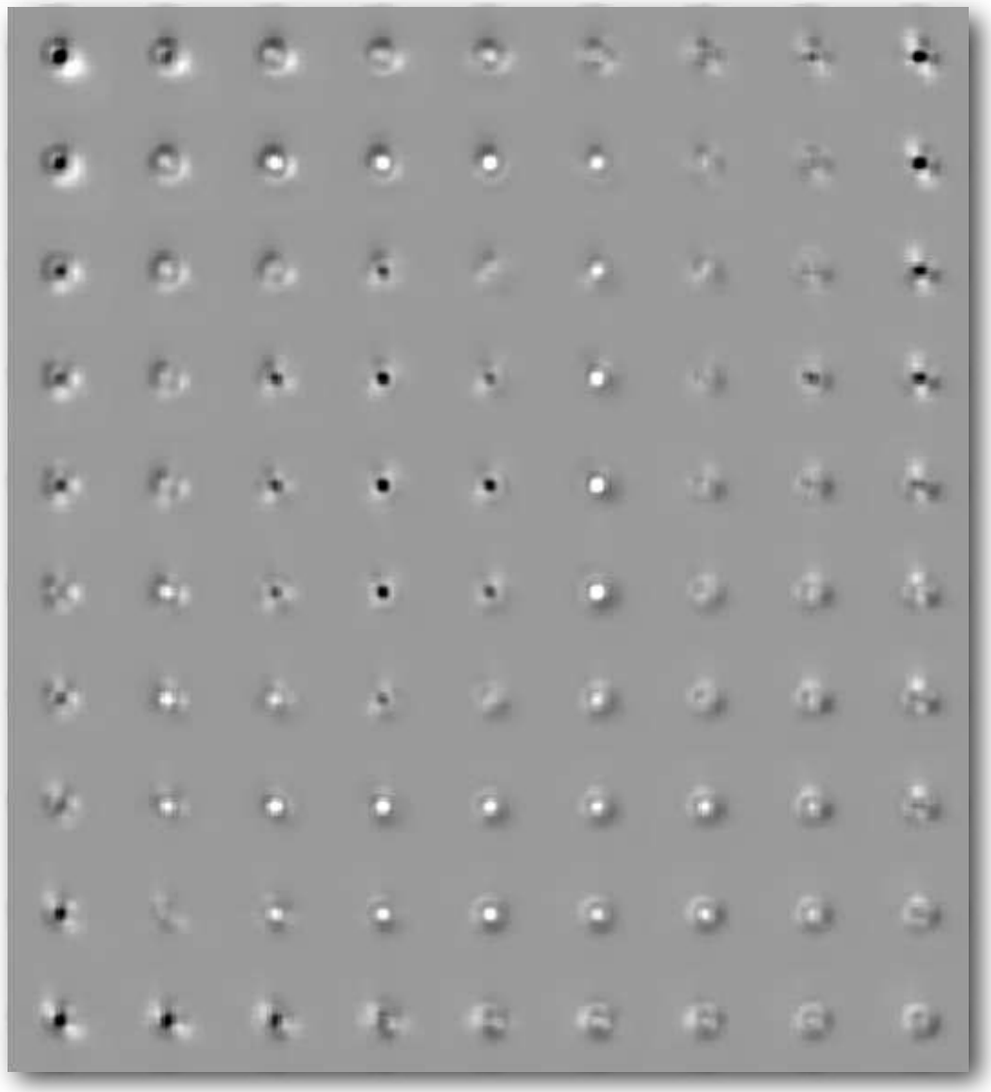

see also Anderson & King ACS ISR2006-1

Surface Brightness Profile Fitting

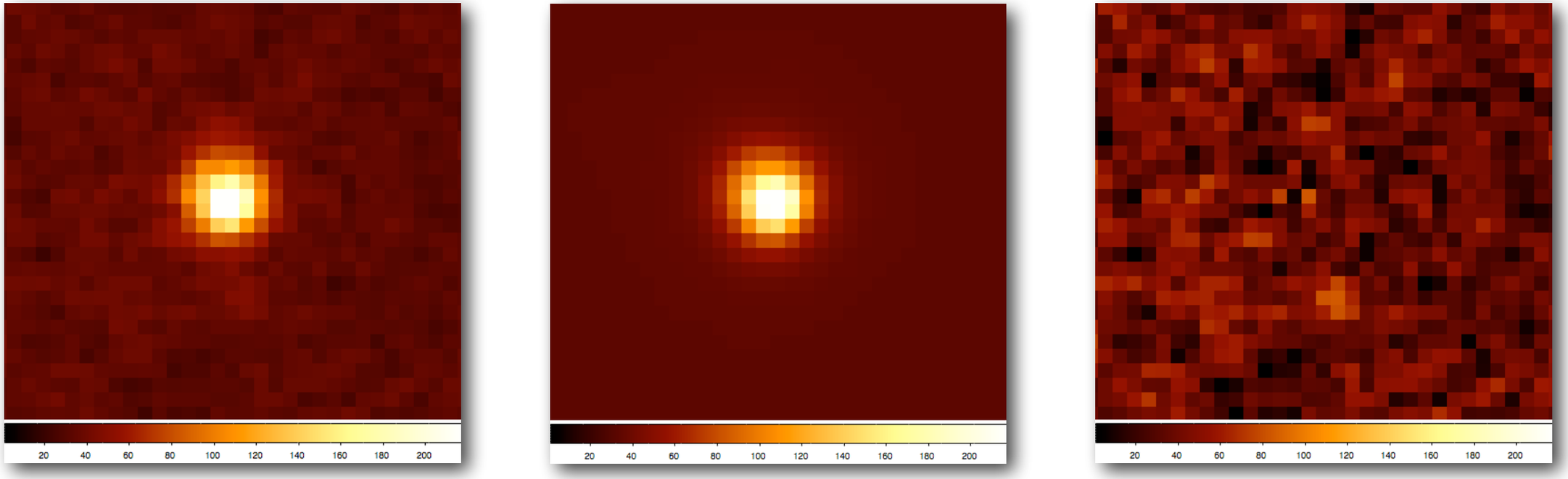

- Modified GalFIT code to fit multiple King profiles and increase efficient processing of multiple profile type combinations
- Objects are marginally resolved, ergo profile cannot be measured directly and has to be assumed
- Tested several profile types: King, Wilson, Elson, Sersic

$$\mu_{\mathrm{K}}(\boldsymbol{r}) = k\left[\left(1+\frac{\boldsymbol{r}^2}{r_c^2}\right)^{-\frac{1}{2}} - \left(1+\frac{r_t^2}{r_c^2}\right)^{-\frac{1}{2}}\right]^2$$

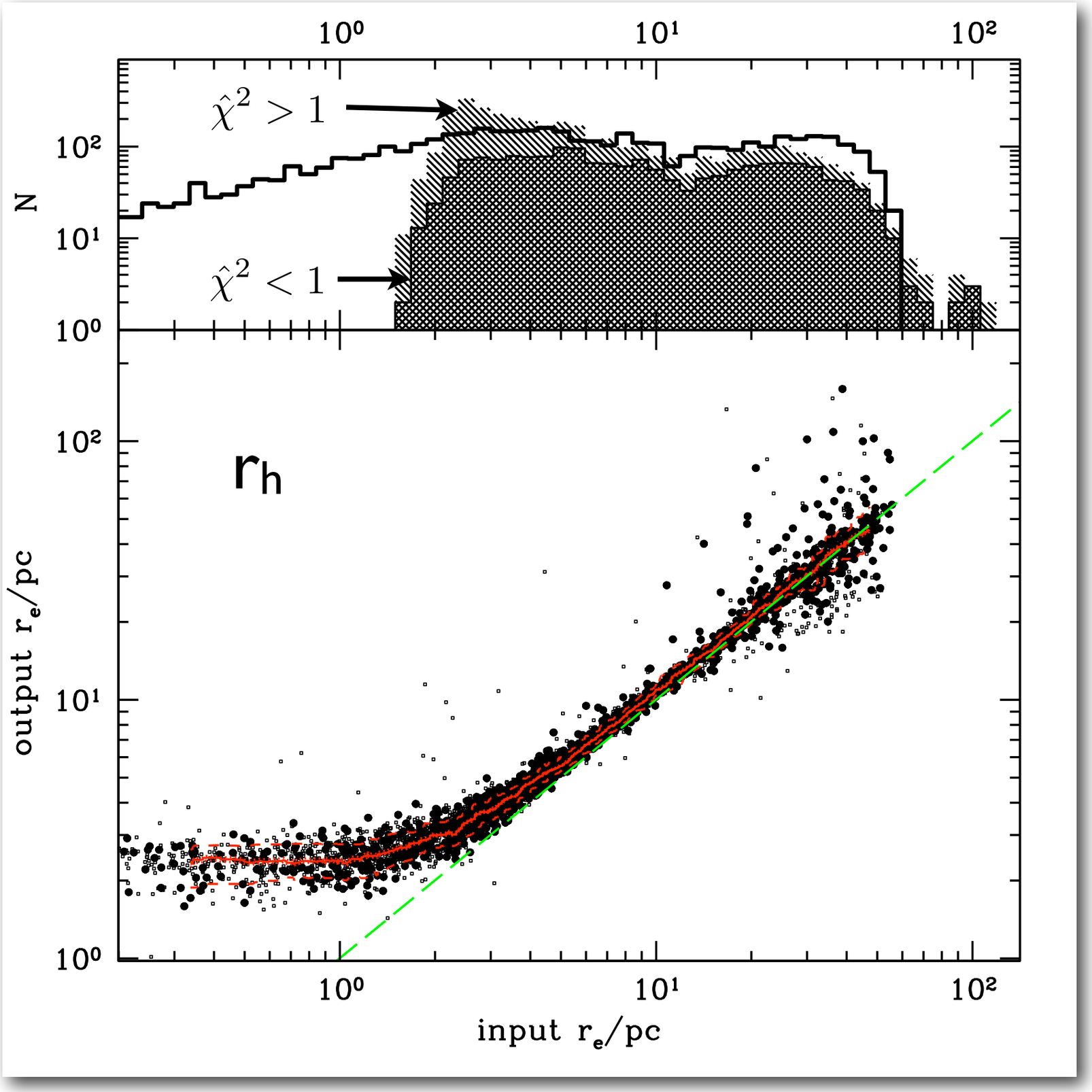
$\hat{\chi}^2 > 1$
$\hat{\chi}^2 < 1$
N
r_h
output r_e/pc
input r_e/pc

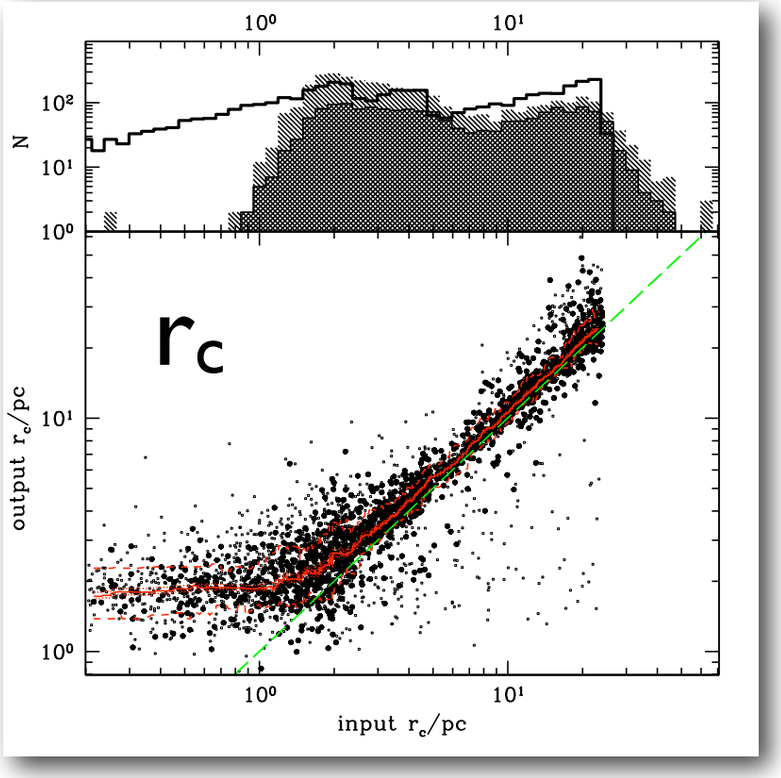
N
r_c
output r_c/pc
input r_c/pc

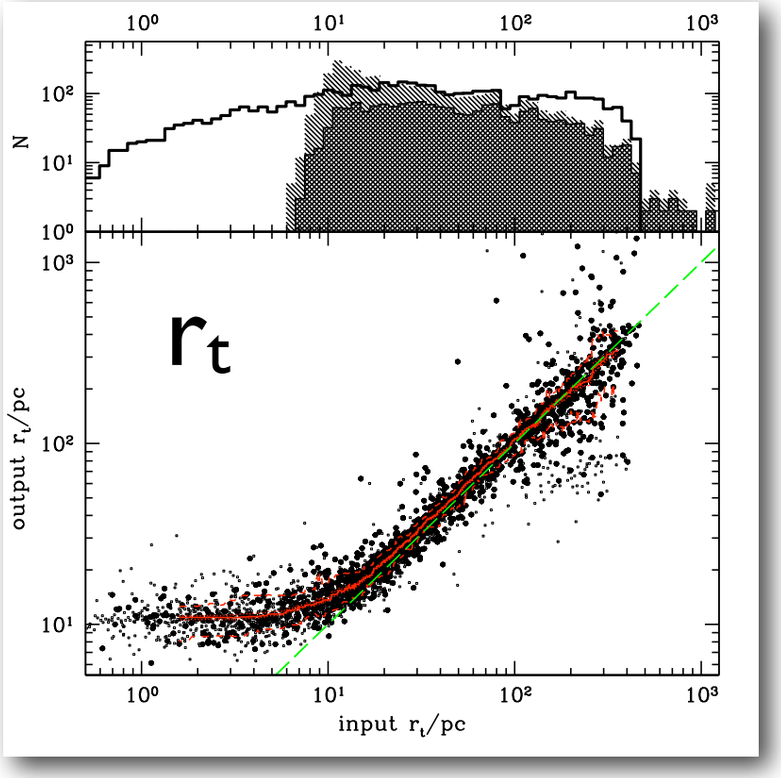
N
r_t
output r_t/pc
input r_t/pc

$$\phi_{r_c} = 0.731 - 5.563 \cdot 10^{-2} r_{c,\mathrm{out}} + 3.742 \cdot 10^{-3} r_{c,\mathrm{out}}^2$$

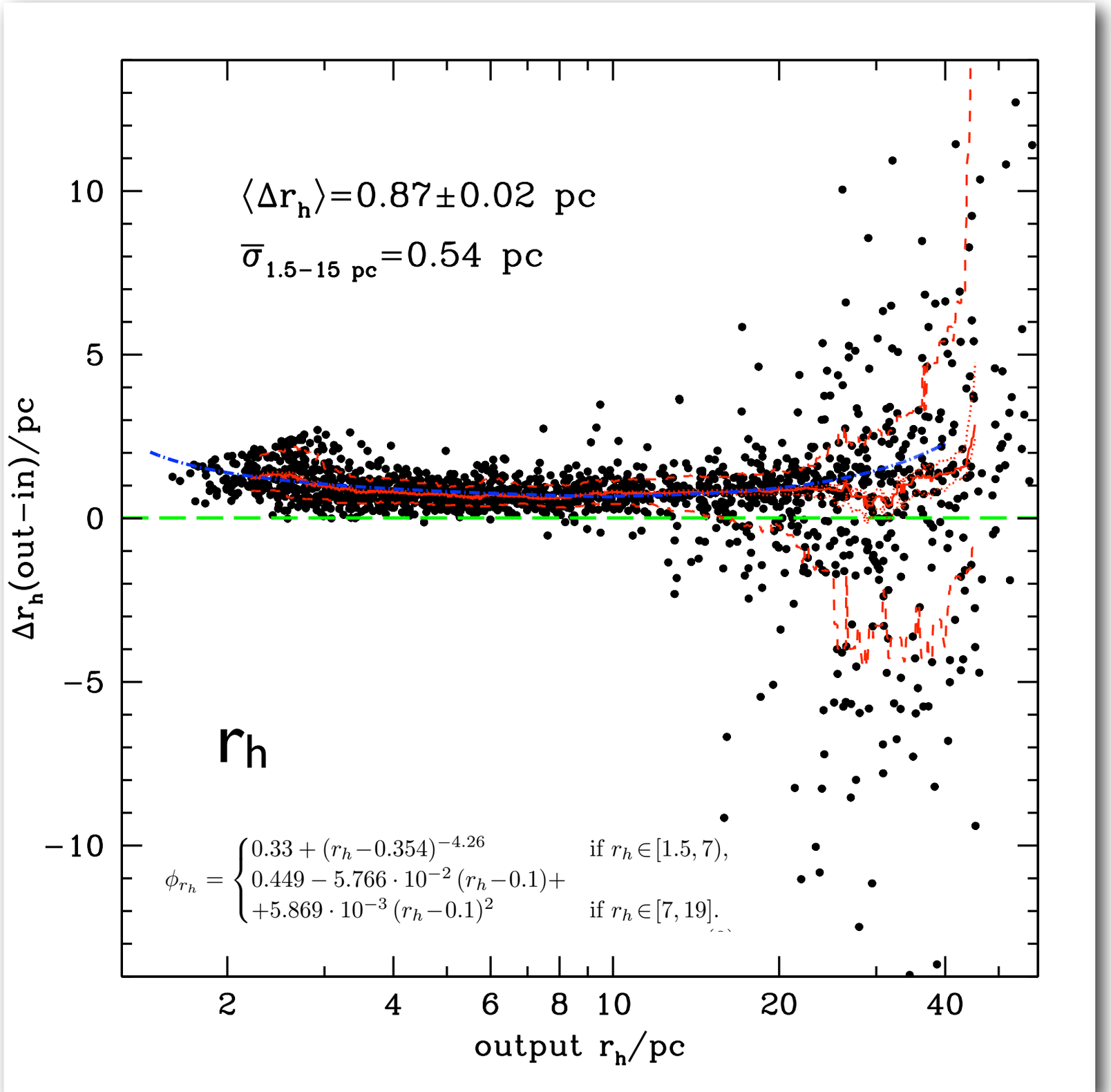

$$\phi_{r_h} = \begin{cases} 0.33 + (r_h - 0.354)^{-4.26} & \text{if } r_h \in [1.5, 7), \\ 0.449 - 5.766 \cdot 10^{-2} (r_h - 0.1) + & \\ +5.869 \cdot 10^{-3} (r_h - 0.1)^2 & \text{if } r_h \in [7, 19]. \end{cases}$$

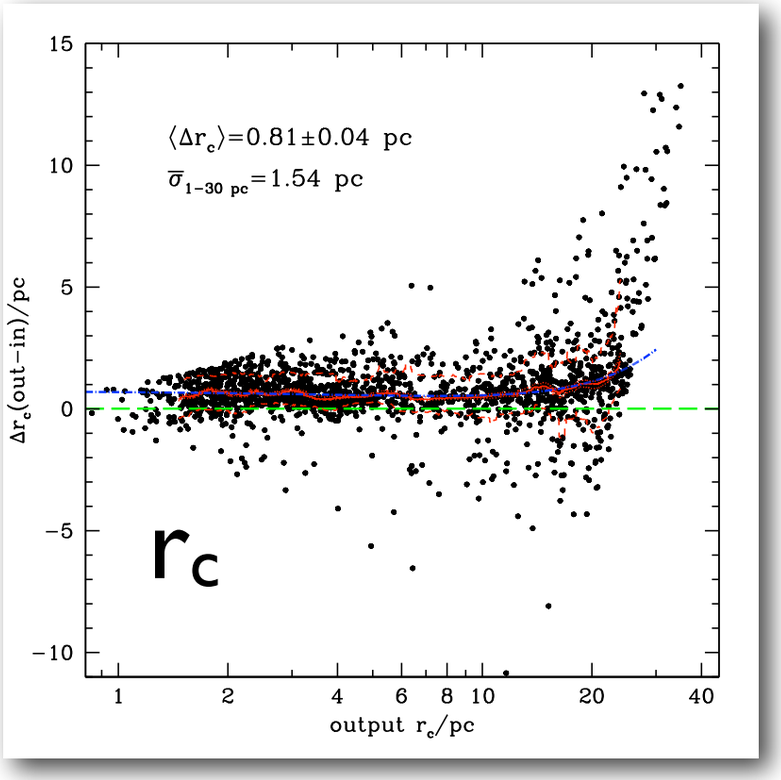

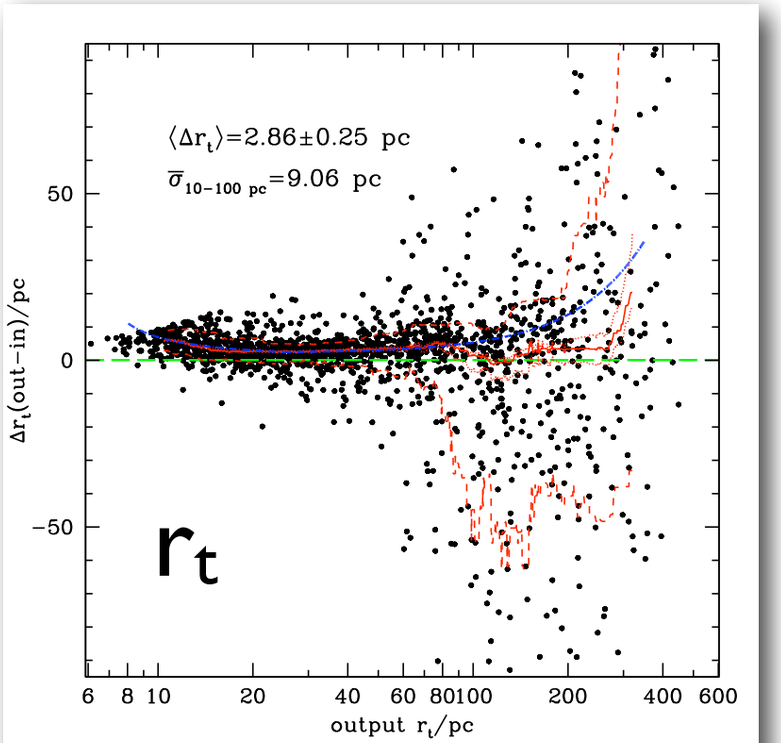

$$\phi_{r_t} = \begin{cases} 0.646 + 22.458 \, (r_t - 5.581)^{-0.86} & \text{if } r_t \in [10, 25), \\ 2.078 + 6.675 \cdot 10^{-3} \, (r_t - 1.11) + & \\ +2.591 \cdot 10^{-4} \, (r_t - 1.11)^2 & \text{if } r_t \in [25, 100], \end{cases}$$

GC half-light radius distributions

TABLE 3
FRACTIONS OF EXTENDED GCS FOR VARIOUS GC SYSTEMS.

Host Galaxy	E_5	$\hat{E}_5$	$R_{\rm gal}$/kpc	$E_{5/10}$	$\hat{E}_{5/10}$	Ref.
NGC 1399	0.122	0.62	51.3	0.061	0.21	(1)
NGC 4486 (M87)	0.066	0.34	12.3	0.065	0.22	(2)
NGC 4472 (M49)	0.073	0.37	11.6	0.072	0.25	(2)
NGC 4594 (M104)	0.026	0.13	15	0.018	0.06	(3)
NGC 5128 (Cen A)	0.170	0.86	20	0.182	0.62	(4)
NGC 224 (M31)	0.151	0.77	150	0.125	0.43	(5)
Milky Way	0.197	$\equiv 1$	120	0.292	$\equiv 1$	(6)

REFERENCES. — (1): this work, (2): ACSVCS, see Jordán et al. (2009), (3): Harris et al. (2010), (4): Woodley & Gómez (2010), (5): Peacock et al. (2009), (6): McMaster catalog, 2010 update of Harris (1996).

NOTE. — $R_{\rm gal}$ is the maximum sampling radius of the corresponding dataset in kpc. While E_5 and $\hat{E}_5$ are the values defined in Equations 12 and 13, the corresponding values for the GC samples restricted to $R_{\rm gal} \leq 10$ kpc are given as $E_{5/10}$ and $\hat{E}_{5/10}$.

$$E_5 = N_{\rm GC}(r_h \geq 5{\rm pc})/N_{\rm GC}({\rm all})$$

$$\hat{E}_5 = \frac{N_{\rm GC}(r_h \geq 5{\rm pc})}{N_{\rm GC}({\rm all})} \left(\frac{N_{\rm GC}(r_h \geq 5{\rm pc})_{\rm MW}}{N_{\rm GC}({\rm all})_{\rm MW}} \right)^{-1}$$

Later-type and isolated galaxies tend to host more extended GCs…

v_{rad} confirmed GCs using data from Schuberth et al. (2010)

Masters et al. (2010)
ACSFCS, central pointing

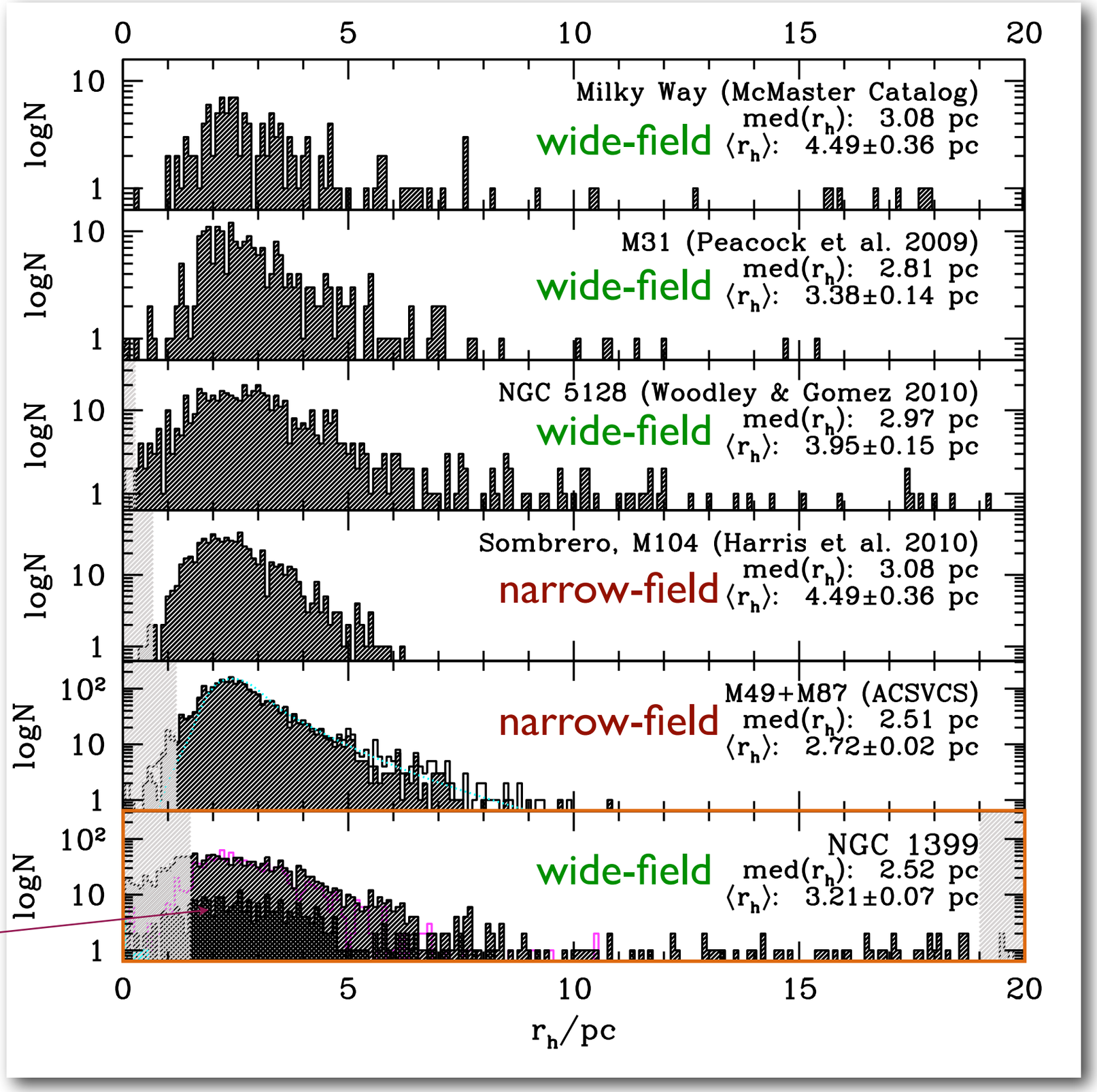

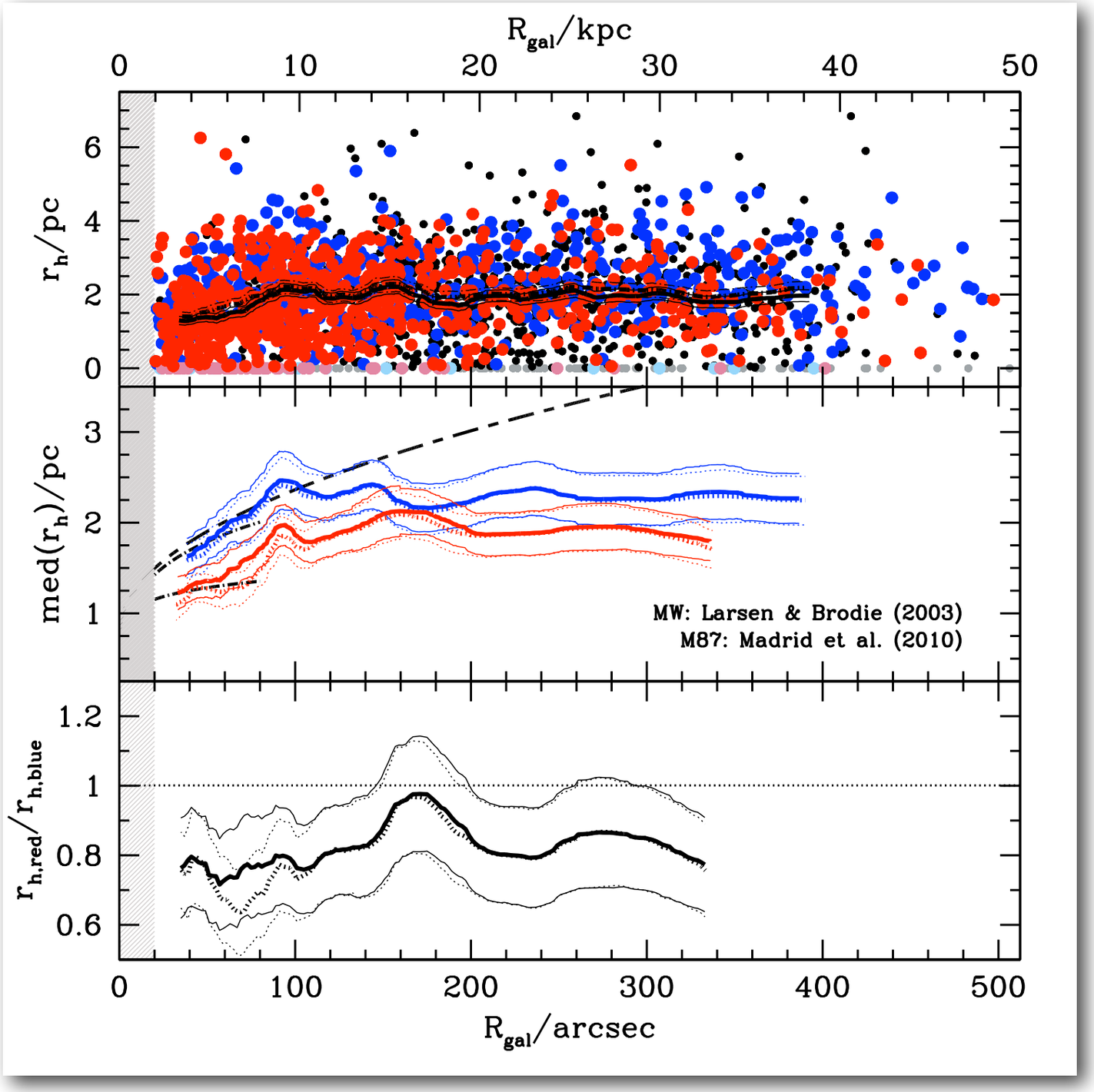

GC Size-Radius Relation

- blue GCs are on average ~20% larger than red GCs at all R_{gal}
- size difference between red and blue GCs present at all R_{gal}!
- cannot be projection effect, but has to be intrinsic to GCs
- trend in inner Fornax regions for red and blue GCs comparable to M87
- blue GC trend comparable to the one of Milky Way GCs

GC *instantaneous* Jacobi radius

stellar+NFW mass

stellar mass

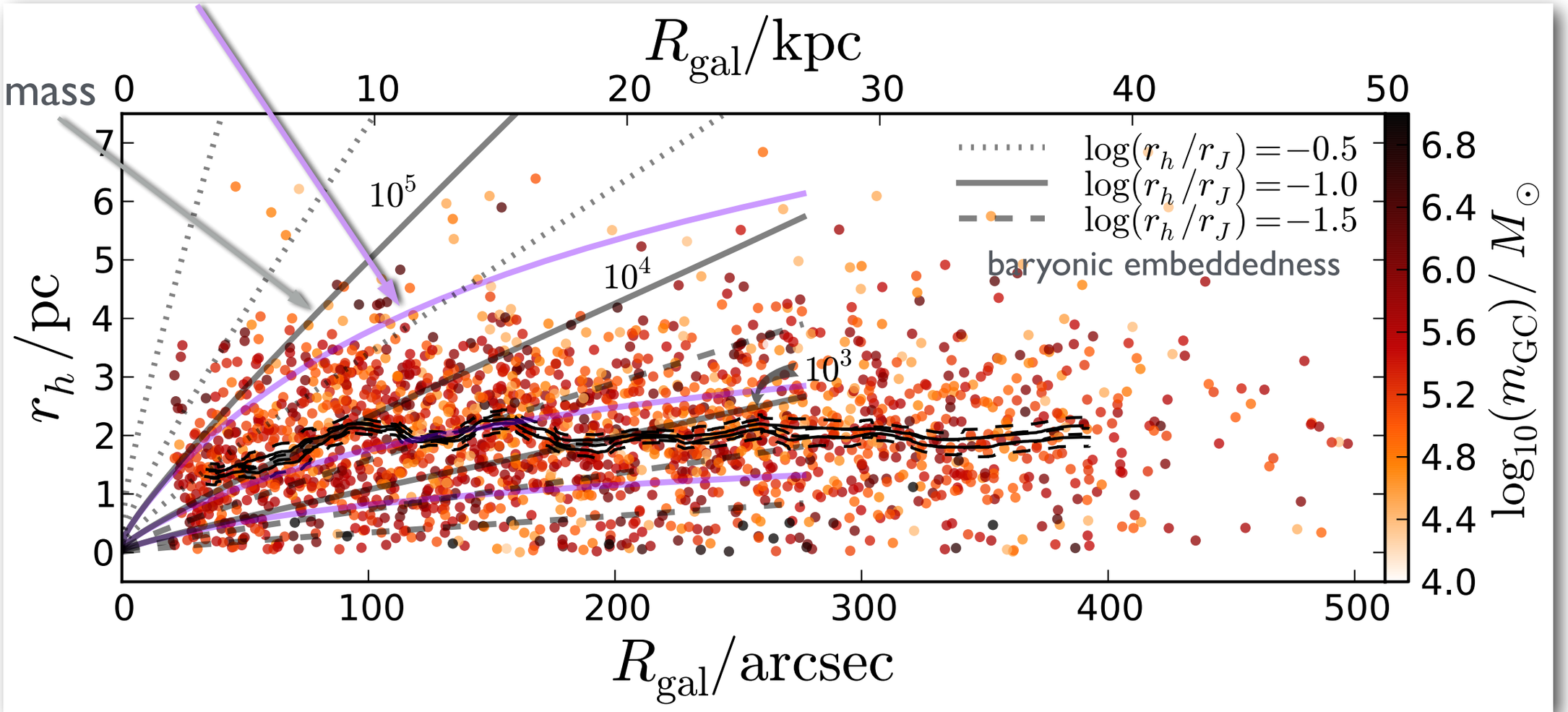

- expectation of radial r_h variation from stellar + NFW mass profile alone are insufficient to explain data ➠ exotic orbit anisotropy f(m_{GC}) or/and harassment by **DM substructure**!